



Comparison of CellSearch versus Parsortix circulating tumor cell enumeration and molecular characterization: A pilot study in metastatic prostate cancer patients

Jenna Kitz ^{a b}, Kelly Seto ^c, Pinki Nandi ^c, Paul Smith ^c, David Englert ^c, Ayten Hijazi ^b,
Michael Lock ^{b d}, Glenn S. Bauman ^{b d}, Scott Ernst ^{b d}, Ricardo Fernandes ^{b d},
Alison L. Allan ^{a b d}  

Show more 

 Outline |  Share  Cite

<https://doi.org/10.1016/j.nexres.2025.100390> 

[Get rights and content](#) 

Under a Creative Commons [license](#) 

Open access

Abstract

Introduction

Prostate cancer is a leading cause of cancer death in men. Although early-stage prostate cancers can be effectively managed by surgery, radiation and/or androgen-deprivation therapies, many tumors eventually become castrate-resistant, leading to disease progression, metastasis and death. The goal of this pilot study was to gain insight into the biology of prostate cancer progression by assessing circulating tumor cells (CTCs) from 3 patient cohorts: low-volume metastatic hormone-sensitive prostate cancer (LV-mHSPC); high-volume metastatic hormone-sensitive prostate cancer (HV-mHSPC); and metastatic castrate-resistant prostate cancer (mCRPC).

Materials & Methods

CTCs were assessed using the epithelial-based CellSearch assay versus an epithelial-to-mesenchymal transition (EMT)-independent Parsortix assay. CTCs were also harvested from Parsortix and assessed by downstream molecular analysis using the HyCEAD mRNA multiplex assay. Specific molecular characteristics identified through HyCEAD were compared to prostate cancer data from The Cancer Genome Atlas (TCGA).

Results

Although no significant enumeration differences were observed between the two technologies, CellSearch was able to identify a greater number of CTCs in HV-mHSPC versus LV-mHSPC patients ($p \leq 0.05$). Between the 3 patient cohorts, 17 differentially expressed genes were identified that may contribute to prostate cancer disease progression.

Conclusions

Taken together, our findings provide a promising panel of potential biomarkers for further investigation in order to develop a comprehensive, real-time CTC liquid biopsy strategy for the personalized clinical management of metastatic prostate cancer patients in the future.



Keywords

Prostate cancer; Epithelial-to-mesenchymal transition (EMT); Circulating tumor cells (CTCs); CellSearch; Parsortix; HyCEAD

GLOSSARY

AKR1C3

Aldo-keto reductase family 1 member C3

AKT1

AKT serine/threonine kinase 1

AR

Androgen receptor

CCNE2

Cyclin E2

CD3D

Cluster of differentiation 3 delta subunit of T-cell receptor complex

CD45

Cluster of differentiation 45

CHAARTED

Chemohormonal therapy versus androgen ablation randomized trial for extensive disease in prostate cancer

CHI3L1

Chitinase 3 like 1

CK

Cytokeratin

CTC

Circulating tumor cell

DAPI

4',6-diamidino-2-phenylindole

EMT

Epithelial-to-mesenchymal transition

EpCAM

Epithelial cell adhesion molecule

ERG

ETS-related gene

FAM107A

Family with sequence similarity 107 member A

FBS

Fetal bovine serum

FDA

Food and Drug Administration

ERMT2

Fermitin family homolog 2

FITC

Fluorescein isothiocyanate

GHR

Growth hormone receptor

HE

High expression

HNV

Healthy normal volunteers

HSREB

Health Sciences Research Ethics Board

HUWE1

HECT, UBA and WWE domain containing E3 ubiquitin protein ligase 1

HV-mHSPC

High-volume hormone-sensitive prostate cancer

HyCEAD

Hybrid capture enrichment amplification and detection

ITGBL1

Integrin beta-like 1 protein

LV-mHSPC

Low-volume hormone-sensitive prostate cancer

MET

Mesenchymal-to-epithelial transition

mCRPC

Metastatic castrate-resistant prostate cancer

NID2

Nidogen-2

NKX3-1

NK3 homeobox 1

NTC

No-template control

PAX8

Paired-box gene 8

PBS

Phosphate-buffered saline

PC

Prostate cancer

PCWG2

Prostate Cancer Clinical Trials Working Group

PE

Phycoerythrin

PPIA

Peptidylprolyl isomerase A

PSA

Prostate-specific antigen

PTPRC

Protein tyrosine phosphatase, receptor type C

RPKM

Reads per kilobase per million mapped reads

RPL4

Ribosomal protein L4

SEPT2

Septin 2

SPARC

Secreted protein acidic and rich in cysteine

ST14

Transmembrane serine protease matriptase

TBP

TATA-box binding protein

TCGA

The Cancer Genome Atlas

TFF1

Trefoil factor 1

TOP2A

Topoisomerase II alpha

VEGF2

Vascular endothelial growth factor 2

VIM

Vimentin

VSTM2L

V-Set and transmembrane domain containing 2 like

ZNF217

Zinc finger protein 217

Introduction

Prostate cancer is the most diagnosed cancer and second most common cause of cancer death in American men [1]. Early-stage prostate cancers are dependent on androgen stimulation for growth, and thus androgen-deprivation therapy by chemical and/or surgical castration is a treatment mainstay for hormone-dependent disease. However, as tumors adapt to the androgen-deprived environment and become castrate-resistant, many patients will experience disease progression. Most deaths from prostate cancer occur because of progressive, castrate-resistant metastatic disease, as current therapies are largely non-curative in this setting [2]. Further insight into the biology of disease progression and metastasis is therefore essential to develop better strategies for treatment. Existing clinical prognostic tools such as Gleason score and/or prostate-specific antigen (PSA) levels are helpful but imperfect for predicting disease outcome, and this uncertainty can result in under-treatment or over-treatment of prostate cancer patients [3]. There is therefore a clear need for improved biomarkers that can be used to accurately select treatments, assess disease progression, and/or evaluate treatment responses. One such biomarker may be circulating tumor cells (CTCs).

The presence of CTCs in the blood of prostate cancer patients has been shown to be an important indicator of metastatic disease and poor prognosis [4]. Additionally, changes in CTC number throughout treatment have been demonstrated to reflect therapy response [5]. Although these cells are very rare (~ 1 CTC per 10^5 - 10^7 leukocytes) [6], recent technological advances facilitate sensitive enumeration and characterization of CTCs. CellSearch (Menarini Silicon Biosystems) [7] was the first FDA-cleared CTC analysis platform, and thus has the greatest amount of clinical outcome data available [8,9]. CellSearch uses an epithelial-based marker approach for immunomagnetic enrichment, isolation, and quantitative immunofluorescence of CTCs. Using this assay, it has been demonstrated that CTCs are readily detectable in ~ 65 % of castrate-resistant prostate cancer (CRPC) patients [9] and that the presence of ≥ 5 CTCs in 7.5 ml of blood is indicative of progressive metastatic disease and reduced overall survival [4]. Notably,

CTCs are undetectable in ~35 % of metastatic CRPC patients using the CellSearch [9]. This suggests that either CTCs are truly not present in >1/3 of patients with advanced metastatic disease, and/or that CTCs are present but not detectable as they do not meet the standard CellSearch definition of CTCs (EpCAM+/Cytokeratin 8/18/19 [CK]+/DAPI+/CD45). Given the accumulating evidence that prostate cancer cells can lose epithelial characteristics and gain mesenchymal characteristics as they evolve towards a more metastatic phenotype [10], we hypothesize that the latter scenario is most likely.

The epithelial-to-mesenchymal transition (EMT) is a critical process during embryonic development and cancer metastasis [11]. Activation of EMT leads to profound phenotypic changes resulting in loss of cell polarity, loss of cell-cell adhesion, resistance to apoptosis, and acquisition of migratory/invasive properties [10,11]. It has also been proposed that tumor cells (via the mesenchymal-to-epithelial transition [MET]) may revert to an epithelial phenotype to facilitate metastatic growth in secondary sites, suggesting a role for phenotypic plasticity during metastatic progression [[10], [11], [12]]. At the molecular level, EMT is mediated by decreased expression of epithelial proteins (e.g., E-cadherin, CK, EpCAM), as well as corresponding increases in mesenchymal factors (e.g., N-cadherin, Vimentin, Twist, Zeb), with MET mediated by the opposite changes [11]. Clinically, Gleason grading can arguably be viewed as morphological evidence of EMT [10], since increasing Gleason score is associated with progressive loss of epithelial architecture, loss of defined basement membrane/cell polarity, and increased invasion [13]. In support of this, studies have demonstrated that decreased expression of E-Cadherin [14] or increased expression of mesenchymal markers (Vimentin, N-Cadherin, Snail) [[15], [16], [17]] in primary prostate tumors is associated with advanced Gleason score, metastasis, and/or poor prognosis. Although the role of androgen receptor (AR) signaling in EMT is poorly understood, studies have also demonstrated that EMT may be facilitated by androgen deprivation [18], castrate-resistance [19], and/or disruption of androgen signaling [20].

Importantly, several clinical studies have demonstrated that CTCs with a purely mesenchymal phenotype are undetectable by CellSearch, but that the presence of mesenchymal marker expression on CTCs with a hybrid epithelial-mesenchymal phenotype is indicative of poor prognosis [12,[21], [22], [23]]. In addition, previous pre-clinical data from our laboratory [24] has revealed that in animal models, prostate cancers with a mesenchymal phenotype shed greater numbers of CTCs more quickly and with greater metastatic capacity than those with an epithelial phenotype. Notably, the clinically used CellSearch-based assay captured most CTCs shed during early-stage disease in vivo, and only after the establishment of metastases were a significant number of CellSearch undetectable CTCs present [24]. Taken together, these clinical and pre-clinical studies suggest that capture and characterization of CTCs with a mesenchymal or hybrid phenotype may be more informative than analysis of those with a purely

epithelial phenotype. To address this challenge, the EMT-independent CTC analysis platform Parsortix has been developed by ANGLE plc [25,26] which can detect CTCs with an epithelial, hybrid, or mesenchymal phenotype. To complement this CTC isolation technology, ANGLE has also developed a sophisticated downstream analysis system for gene expression profiling of cells called HyCEAD (Hybrid Capture Enrichment Amplification and Detection), which allows for the simultaneous multiplex analysis of 100+ mRNA species [27,28].

In the current pilot study, we tested the hypothesis that patients at later stages of prostate cancer progression will have a greater number of CTCs with enhanced EMT characteristics. We investigated this in prostate cancer patients at different disease progression stages along the spectrum of hormone-sensitive to castrate-resistant metastatic disease. We assessed and compared patient CTCs using the epithelial-based CellSearch clinical assay versus our in-house developed and validated EMT-independent Parsortix CTC protocol combined with molecular characterization by HyCEAD. Our findings highlight a promising panel of potential biomarkers that have the potential to be used alone or as a molecular signature to develop a comprehensive, real-time CTC liquid biopsy strategy for the personalized clinical management of metastatic prostate cancer patients in the future.

Materials & Methods

Patient population

All studies were carried out under a protocol approved by the Western University Health Sciences Research Ethics Board (HSREB; protocol #109759) and performed in accordance with all relevant HSREB guidelines and regulations, including obtaining informed consent from all participants. The study was conducted as a single-center observational clinical trial of metastatic prostate cancer patients at different disease progression stages along the spectrum of hormone-sensitive to castrate-resistant (ClinicalTrials.Gov #NCT04021394). A total of 29 evaluable patients were accrued at the London Health Sciences Centre (London, ON Canada) following informed consent. Patients were accrued based on 3 progressive disease stage cohorts including (1) Low-volume metastatic hormone-sensitive prostate cancer (LV-mHSPC) [29] ($N = 10$ patients); (2) High-volume metastatic hormone-sensitive prostate cancer (HV-mHSPC) [29] ($N = 9$ patients); and (3) Metastatic castrate-resistant prostate cancer (mCRPC) [30] ($N = 10$ patients). All patients were 18 years of age or older with histologically diagnosed prostate cancer and documented evidence of metastatic disease. Specific inclusion criteria for the LV-mHSPC cohort: previous treatment with androgen deprivation therapy for <90 days and/or recommended but not yet started new line of androgen deprivation therapy; and bone

only metastatic disease (<4 lesions contained within vertebral column or pelvis) [29]. Inclusion criteria for the HV-mHSPC cohort: previous treatment with androgen deprivation therapy for <90 days and/or recommended but not yet started new line of androgen deprivation therapy; and visceral metastases (extranodal) and/or bone metastases (≥ 4 bone lesions with ≥ 1 lesion outside vertebral column or pelvis) [29]. Inclusion criteria for the mCRPC cohort: documented evidence of progression while receiving androgen ablation therapy (medical or surgical castration) according to PCWG2 criteria; and bone and/or visceral metastatic disease [30].

Blood collection and CTC enumeration

Blood samples (2×10 mL) were collected from each patient by routine phlebotomy into CellSave preservative blood collection tubes (Menarini Silicon Biosystems, Huntingdon Valley, PA, USA) for pre-analytical stabilization of CTCs for up to 96 hours. One blood sample (7.5 mL) was analyzed by CellSearch (Menarini Silicon Biosystems) and CTCs were enumerated based on an EpCAM+/CK+/CD45-/DAPI+ cell phenotype as previously described [31]. The second blood sample (7.5 mL) was analyzed using Parsortix (ANGLE plc, Guildford, UK) as described previously [32], using 6.5 μm cassettes. CTCs were enumerated based on the standard Parsortix in-cassette staining protocol with the addition of a custom antibody panel [32]. In reagent tubes one and two, 1–2 mL of flow buffer, consisting of phosphate buffer solution (PBS) and 3 % fetal bovine serum (FBS), was added in place of 4 % paraformaldehyde fixative and permeabilization reagents, respectively. Reagent tube three consisted of 1 mL flow buffer and 10 μL anti-human N—Cadherin- PE (Invitrogen, 12–3259–42, Waltham, MA, USA), 20 μL anti-Human EpCam- PE (BD, 347,198, Franklin Lakes, NJ, USA), 20 μL anti-Human CD45-FITC (Beckman Coulter, IM0782U, Brea, CA, USA), and 5 μL DAPI (Sigma Aldrich, Ref: D9542, St. Louis, MO, USA). Reagent tube three and the cassette holder were covered in aluminum foil to protect antibodies from light during CTC staining. EpCAM and N—Cadherin antibodies were both labeled with the same fluorochrome to identify CTCs regardless of EMT phenotype. EpCAM+ or N—Cadherin+/CD45-/DAPI+ cells were considered positive CTCs.

RNA isolation and HyCEAD analysis

Following enumeration, CTCs were collected via the Parsortix platform's harvest protocol into 1.5 mL RNase/DNase-free microtubes (Diamed, Mississauga, ON, Canada) per patient sample as previously described [32]. Isolated CTCs were centrifuged at 700 x g for 10 min, supernatants were discarded without disturbing the pellet, and CTCs were lysed via manual pipetting using 50 μL lysis/binding buffer from the Dynabeads mRNA Purification Kit (Thermo Fisher, 61,021). Harvested CTCs in lysis/binding buffer were stored at -80 °C prior to analysis. HyCEAD mRNA analysis was performed as described previously [27,28]. Briefly, polyA⁺ mRNA was captured directly from cell lysates and subjected to multiplex

amplification and labeling of targeted sequences for each gene of interest. Products were sorted and quantified by chemiluminescent detection on flow-through chips. Two gene expression chips including the prostate cancer (“PC”) chip and the high expression (“HE”) chip were developed by ANGLE and previously validated on a separate mCRPC patient cohort [28]. The specific genes contained within each expression chip are shown in *Supplemental Table S2*. Automated analysis was completed based on signal intensity compared to control cell/tissue RNA. Genes identified during HyCEAD analysis were considered significantly upregulated if they had signal intensities of >20-fold compared to the average signal intensities of non-template controls (NTC) and healthy normal volunteers (HNV).

TCGA analysis

Follow-up analysis on upregulated genes identified via HyCEAD was completed using online patient data from The Cancer Genome Atlas (TCGA). Using the gene analysis UALCAN database [33] (last accessed on December 12/2021), each gene with altered expression between clinical groups was analyzed. Utilizing the TCGA dataset, genes were assessed for changes in expression in prostate adenocarcinoma versus normal tissues and metastatic prostate cancer versus non-metastatic prostate cancer (MET500 dataset) as well as correlation with overall survival.

Data analysis

Statistical analysis was completed using GraphPad Prism 9 for MacOS (San Diego, CA, US). All data are presented as the mean \pm standard deviation (SD) unless noted otherwise. For matched samples, two-tailed non-parametric Wilcoxon matched-pairs signed rank tests were performed. For analysis between patient groups non-paired, non-parametric Kruskal-Wallis tests, with Dunn’s multiple comparisons follow up tests were performed. For all experiments, $p \leq 0.05$ was considered statistically significant.

Results

Patient characteristics

Metastatic hormone-sensitive prostate cancer (mHSPC) is diagnosed when a patient’s cancer has spread from the primary site to other parts of the body but can still be treated with hormone deprivation therapy to block, stop, or slow cancer growth [29]. Bone is the most common site of metastasis in patients with prostate cancer [34]. Based on CHAARTED criteria [29] high volume hormone-sensitive prostate cancer (HV-mHSPC) includes 4 or more bone lesions (at least 1 lesion outside of the vertebral column and pelvis) and/or visceral metastasis, which indicates poorer prognosis compared to low

volume hormone-sensitive prostate cancer (LV-mHSPC) patients. We therefore assessed patients with both LV-mHSPC ($N = 10$) and HV-mHSPC ($N = 9$). In addition, we included patients with metastatic castrate-resistant prostate cancer (mCRPC, $N = 10$). Despite androgen deprivation therapy, these patients develop disease progression in the setting of castrate testosterone levels, e.g., increased tumor size on imaging and/or rising PSA levels. Patients with mCRPC may undergo systemic chemotherapy, androgen receptor-axis-targeted therapies, radiopharmaceutical compounds, and/or radiation targeted at primary/metastatic sites, however there are currently no curative therapies in this setting and the range of survival for CRPC is only 9–36 months. As such, mCRPC represents the disease stage where prostate cancer patients have the poorest prognoses and/or the most impaired quality of life [30].

Study population characteristics are summarized in [Table 1](#). In all three cohorts, the majority of patients (72.4 %) had a Gleason score of >6 . Average serum PSA levels in each patient cohort were 22.0 $\mu\text{g/L}$ (LV-mHSPC), 131.7 $\mu\text{g/L}$ (HV-mHSPC), and 99.1 $\mu\text{g/L}$ (mCRPC). The most common site of metastasis across all cohorts was bone, with 86.2 % of patients having ≥ 1 bone metastasis. For the LV-mHSPC group, most patients had 2 different sites of bone metastasis (spine and pelvis), whereas in the HV-mHSPC group the majority of patients had 5–8 different sites of bone metastases, including spine, pelvis, ribs, skull, shoulder, femur, humerus, hip, sternum, and/or clavicle. In all cohorts, the majority of patients had 0–5 lesions per anatomical sites of bone metastasis. Of patients in the HV-mHSPC and mCRPC cohorts, 63.2 % had metastases to the lymph node. In these two more advanced cohorts, 47.4 % had visceral metastasis and the majority (with a known number of metastatic lesions) had 1 lesion per anatomical site of visceral metastasis, which included lung, liver, pelvic wall, orbit, adrenal, spleen, kidney, bladder, an/or esophagus.

Table 1. Patient Characteristics at Time of Enrollment.

	LV-mHSPC ($N = 10$)	HV-mHSPC ($N = 9$)	mCRPC ($N = 10$)	Total ($N = 29$)
Gleason score^a				
≤ 6	2	1	4	7 (24.1 %)
7	2	3	2	7 (24.1 %)
8	2	2	0	4 (13.8 %)
9	3	3	4	10 (34.5 %)
Unknown	1	0	0	1 (3.4 %)

	LV-mHSPC (N = 10)	HV-mHSPC (N = 9)	mCRPC (N = 10)	Total (N = 29)
Serum PSA (ug/L)				
0.5–10	6	2	1	9 (31 %)
11–50	1	2	3	6 (20.7 %)
51–100	1	1	2	4 (13.8 %)
101–600	1	3	2	6 (20.7 %)
Unknown	1	1	2	4 (13.8 %)
Bone metastasis (BM)	10	9	9	28 (96.6 %)
# of distinct sites^{b, c} of BM				
0	0	0	1	1 (3.4 %)
1	3	0	0	3 (10.3 %)
2	7	1	4	12 (41.4 %)
3	0	1	0	1 (3.4 %)
4	0	1	1	2 (6.9 %)
5	0	2	0	2 (6.9 %)
6	0	3	3	6 (20.7 %)
8	0	1	1	2 (6.9 %)
# of total lesions/patient of BM				
0–5 lesions	10	1	4	15 (51.7 %)
6–10 lesions	0	5	4	9 (31.0 %)
>10 lesions	0	3	2	5 (17.2 %)
Metastasis to lymph node	Not applicable ^d	7	5	12 (41.4 %)
Visceral metastasis (VM)	Not applicable ^d	4	5	9 (31.0 %)
# of distinct sites^{b, d} of VM				
0	Not applicable ^d	5	5	10 (34.5 %)
1	Not applicable ^d	2	5	7 (24.1 %)
2	Not applicable ^d	2	0	2 (6.9 %)
# of total lesions/patient of VM	Not applicable ^d			

	LV-mHSPC (N = 10)	HV-mHSPC (N = 9)	mCRPC (N = 10)	Total (N = 29)
0 lesions		4	5	9 (31.0 %)
1 lesion		2	4	6 (20.7 %)
2 lesions		2	1	3 (10.3 %)
4 lesions		1	0	1 (3.4 %)

a

Derived from needle biopsy.

b

Site refers to a unique location of distance metastasis (e.g., spine, hip, femur, lung, liver, etc.).

c

Specific bone metastasis sites included spine ($n = 66$ total lesions), pelvis ($n = 37$ total lesions), ribs ($n = 22$ total lesions), skull ($n = 12$ total lesions), shoulder ($n = 9$ total lesions), femur ($n = 8$ total lesions), humerus ($n = 7$ total lesions), hip ($n = 6$ total lesions), sternum ($n = 5$ total lesions), and clavicle ($n = 2$ total lesions).

d

Specific visceral metastasis sites included lung ($n = 6$ total lesions), liver ($n = 2$ total lesions), and pelvic wall, orbit, adrenal, spleen, kidney, bladder, and esophagus ($n = 1$ lesion each).

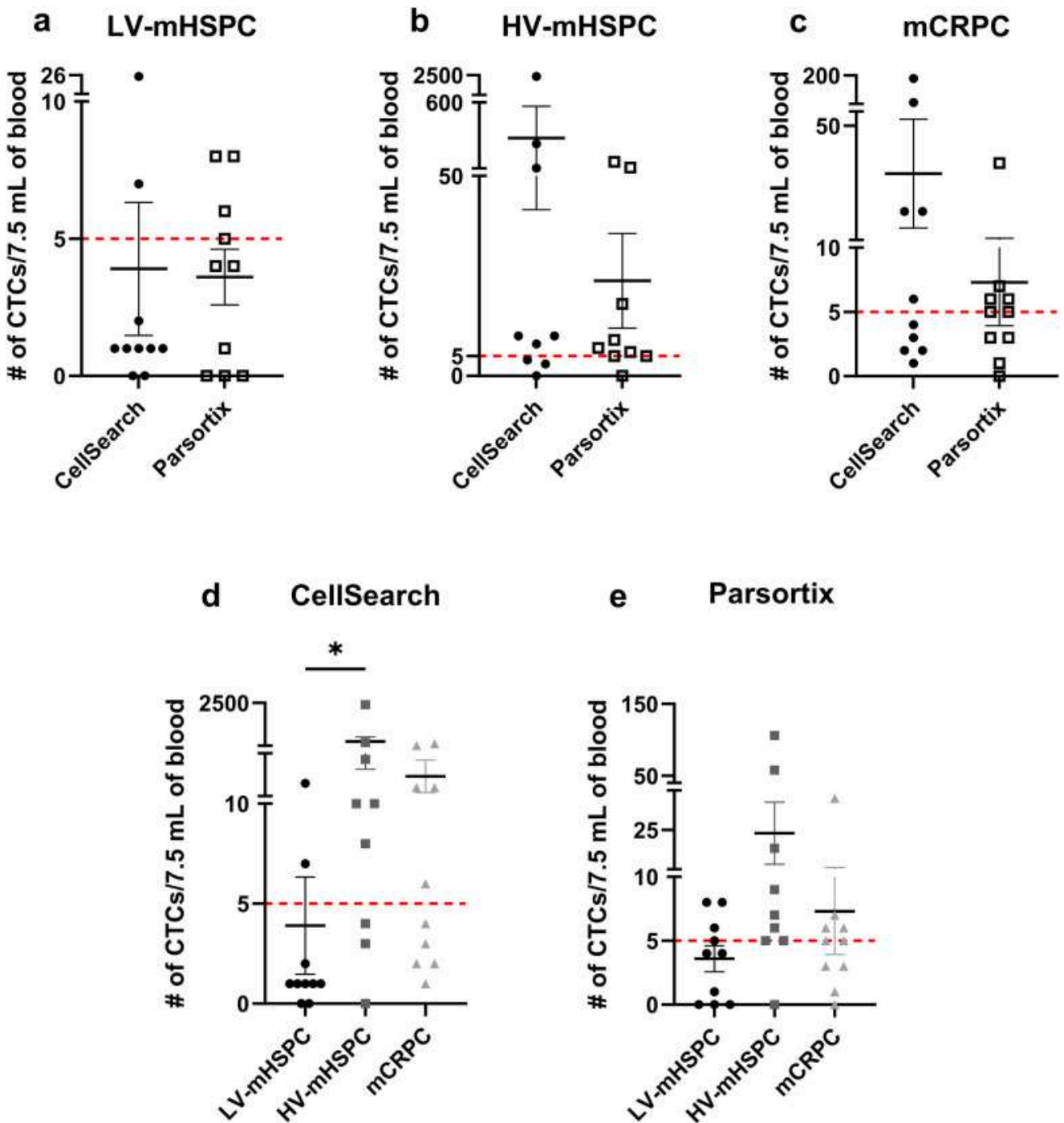
d

Inclusion criteria for the LV-mHSPC group is bone-only metastatic disease, so these patients did not have lymph node or visceral metastases.

CTC enumeration in metastatic prostate cancer patients is similar between CellSearch and Parsortix

We were first interested in determining if there were differences in CTC enumeration ability between CellSearch versus Parsortix in metastatic prostate cancer patients with increasingly progressive disease. In the LV-mHSPC cohort ($N = 10$ patients), we observed a mean of 3.9 ± 7.7 CTCs with CellSearch and a mean of 3.6 ± 3.2 CTCs with Parsortix ([Fig. 1a](#)). In the HV-mHSPC cohort ($N = 9$ patients), we observed a mean of 305.1 ± 790.6 CTCs with CellSearch and 23.8 ± 35.4 CTCs with Parsortix ([Fig. 1b](#)). In the mCRPC cohort ($n = 10$ patients), we observed a mean of 33.3 ± 60.3 CTCs with CellSearch and 7.3 ± 10.7 CTCs with Parsortix ([Fig. 1c](#)). We did not observe any statistical differences in CTC number between CTC platforms in any of the three patient cohorts ([Fig. 1a-c](#)). However, in the

HV-mHSPC and mCRPC cohorts (*Fig. 1b,c*) we did observe a trend towards higher CTC numbers using CellSearch versus Parsortix, which was somewhat contradictory to our original hypothesis. In addition, the presence of ≥ 5 CTCs in 7.5 ml of blood has previously demonstrated to be prognostic for progressive metastatic disease and reduced overall survival in prostate cancer using CellSearch [4], with the horizontal red lines in *Fig. 1* identify this 5 CTC cut-off on the y-axis. While this observation suggests the possibility that CellSearch may perform better than Parsortix for CTC enumeration, this should be interpreted cautiously since the prognostic CTC enumeration threshold often differs between technologies and has not yet been defined for Parsortix.



[Download: Download high-res image \(613KB\)](#)

[Download: Download full-size image](#)

Fig. 1. CTC recovery in metastatic prostate cancer patients is similar between CellSearch and Parsortix but CellSearch identifies the presence of increased CTCs in HV-mHSPC versus LV-mHSPC prostate cancer patients. Whole blood samples (7.5 ml) were collected from prostate cancer patients after informed consent and analyzed for CTCs using CellSearch and Parsortix as described in the Materials and Methods. (a) LV-mHSPC cohort ($N = 10$); (b) HV-mHSPC cohort ($N = 9$); and (c) mCRPC cohort ($N = 10$). (d-e) Comparison between LV-mHSPC, HV-mHSPC, and mCRPC cohorts ($n = 9-10$ /cohort) using the (d) CellSearch or (e) Parsortix platforms for CTC enumeration. * = significantly different between patient cohorts ($p \leq 0.05$). Red line indicates pre-established CellSearch prognostic cut-off of ≥ 5 CTCs. Individual patient CTC numbers using CellSearch and Parsortix are summarized in *Supplemental Table S1*.

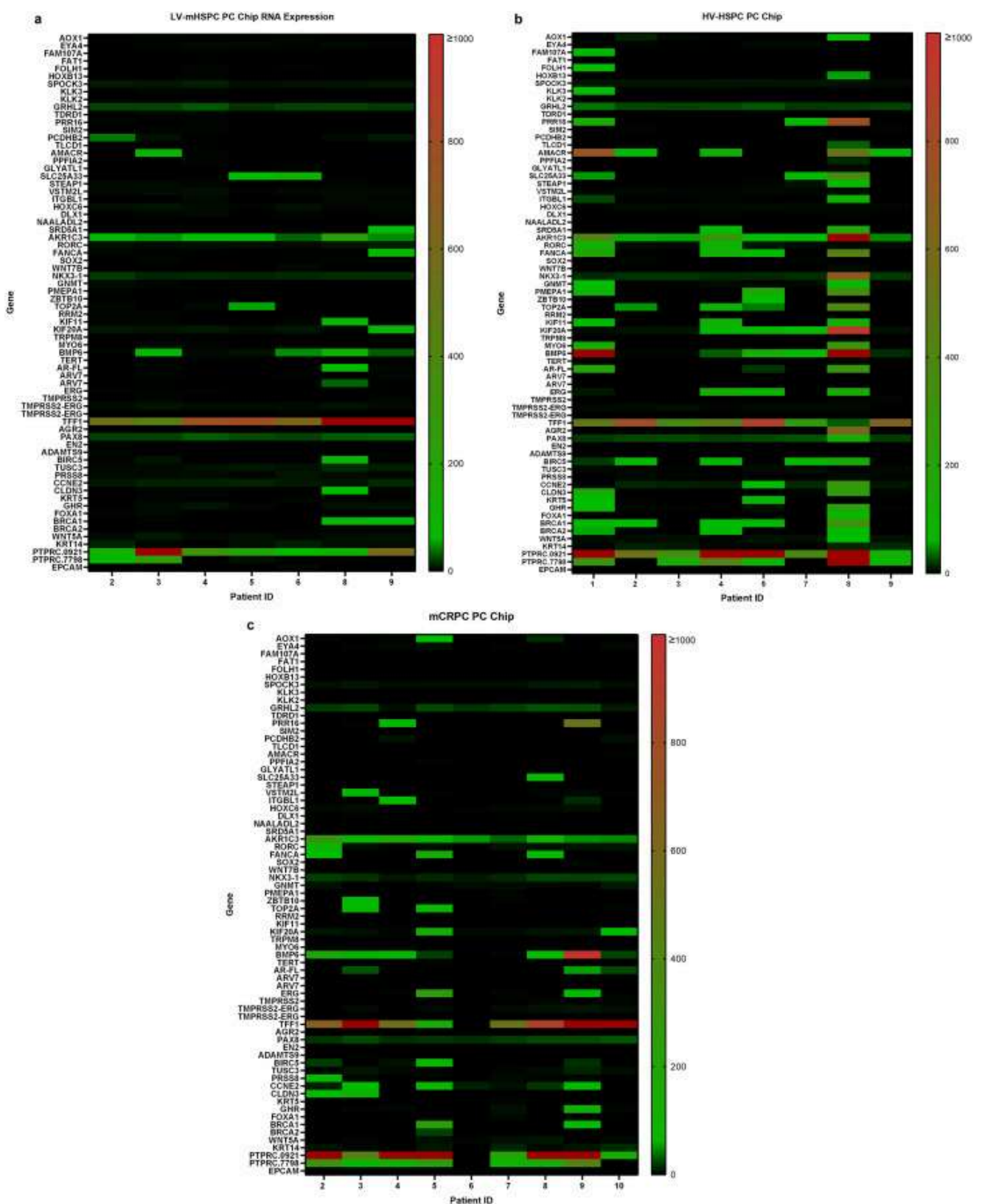
CellSearch identifies the presence of increased CTCs in HV-mHSPC versus LV-mHSPC patients

We next assessed whether there were differences in the number of CTCs present between disease cohorts assessed by the same CTC analysis platform. We observed that there were significantly more CTCs identified in the HV-mHSPC cohort versus the LV-mHSPC group using CellSearch ($p \leq 0.05$) (*Fig. 1d*). No significant differences between CTC number were observed between disease cohorts analyzed with Parsortix (*Fig. 1e*). Individual patient CTC numbers using CellSearch and Parsortix are summarized in *Supplemental Table S1*.

HyCEAD chip analysis identifies differential expression of 119 genes across metastatic prostate cancer patient cohorts

Although no major differences were observed between CTC platforms in terms of ability for CTC enumeration, Parsortix possesses an advantage over CellSearch whereby CTCs can be easily harvested for downstream molecular analysis. In combination with ANGLE's HyCEAD technology [27,28], this presents the opportunity to assess the expression of unique mRNA species across all three patient cohorts to identify potential molecular markers of metastasis and/or EMT. Pre-analytical variables related to the influence of the preservative in CellSave tubes (used in this study) versus EDTA tubes used in the original development of HyCEAD [27] on mRNA capture were first compared to validate the ability to accurately analyze mRNA from CTCs collected in CellSave tubes prior to assessing patient samples. Relative signal intensities (SI) of the detected probes were similar at low signal levels between the two tubes, although at higher SI, samples collected in CellSave tubes showed slightly lower signal compared to EDTA tubes. Time between blood collection and Parsortix CTC isolation did not appear to have a significant impact on efficacy of HyCEAD analysis (*Supplemental Figure S1*). Based on this, we proceeded with patient analysis.

HyCEAD analysis using both Prostate Cancer (PC) and High Expression (HE) chips (*Supplemental Table S2*) identified a total of 119 genes with increased expression in at least 1 patient across the 3 patient sample cohorts and 2 expression chips, where a > 20-fold increase in signal intensity compared to the no-template control (NTC) was considered significant. This included 49 genes identified using the PC chip (*Fig. 2* and *Supplemental Tables S2, S3*) and 70 additional genes identified with the HE chip (*Fig. 3* and *Supplemental Tables S2, S4*) ($n \geq 7$ /cohort). Heatmap visualization of the gene expression data on an individual patient basis revealed that 4 genes on the PC chip (AKR1C3, PAX8, PTPRC and TFF1; *Fig. 2*) and 5 genes on the HE chip (NID2, PPIA, RPL4, SPARC and VIM; *Fig. 3*) were overexpressed (>20-fold) in the majority of patients across all patient cohorts. In addition, 5 genes on the HE chip were overexpressed (>20-fold) in the majority of HV-mHSPC patients only, including AKT1, CD3D, CHI3L1, HUWE1, and SEPT2 (*Fig. 3b*). Interestingly, the HV-mHSPC cohort displayed the greatest heterogeneity of gene expression changes between patients, and overall the HV-mHSPC cohort had the greatest number of total altered transcripts (103 genes) followed by the mCRPC cohort (89 genes) and the LV-mHSPC cohort (69 genes) (*Figs. 2,3* and *Supplemental Figure S2*).

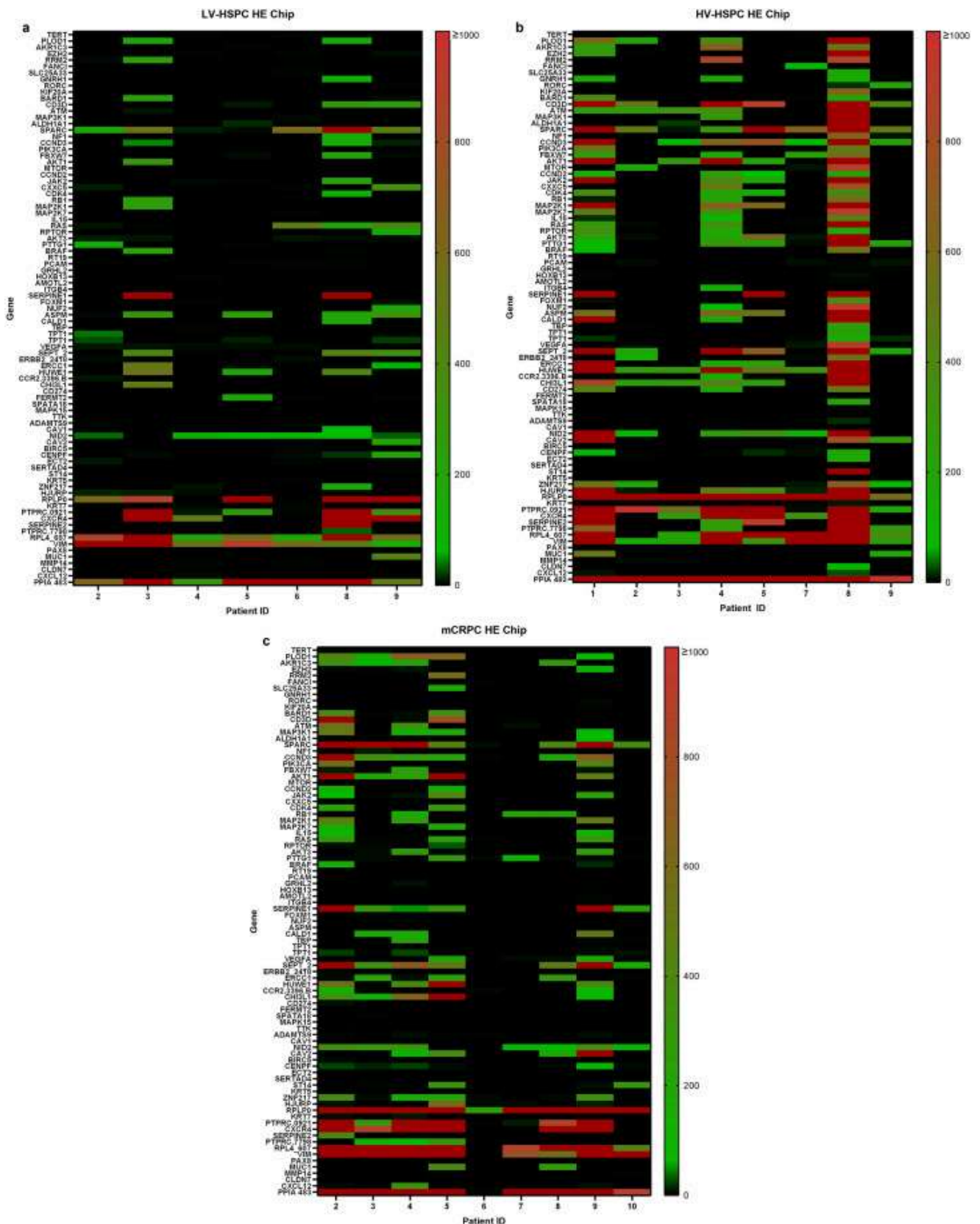


[Download: Download high-res image \(1MB\)](#)

[Download: Download full-size image](#)

Fig. 2. HyCEAD PC chip analysis identified 49 genes with increased expression in the three metastatic prostate cancer patient cohorts. Patient CTCs were isolated using Parsortix via the harvest protocol and dissolved in Dynabead RNA lysis buffer as a pooled CTC population for each individual patient. CTC samples were assessed for RNA expression using HyCEAD and Zplex chip technology (ANGLE plc). Heatmaps were used

to display the expression of individual genes for each patient. Genes identified during HyCEAD analysis were considered significantly upregulated if they had signal intensities of >20-fold higher than the average no-template control (NTC) gene amplification and were assigned a green color gradient (up to a change of 999-fold), with genes with signal intensities of ≥ 1000 -fold higher than NTC were assigned a red color gradient. Genes with signal intensities <20-fold higher than NTC were not considered significantly upregulated and were assigned a black color. (a-c) HyCEAD prostate cancer (PC) chip analysis identified increased expression of genes (*green to red gradient*) in all three cohorts compared to NTC control, including (a) 21 genes in the LV-mHSPC cohort ($n = 7$ patients with CTCs); (b) 36 genes in the HV-mHSPC cohort ($n = 8$ patients with CTCs); and (c) 20 genes in the CRPC cohort ($n = 9$ patients with CTCs).



[Download: Download high-res image \(1MB\)](#)

[Download: Download full-size image](#)

Fig. 3. HyCEAD high expression (HE) chip analysis identified 70 genes with increased expression in the three metastatic prostate cancer patient cohorts. Patient CTCs were isolated using Parsortix via the harvest protocol and dissolved in Dynabead RNA lysis buffer as a pooled CTC population for each individual patient. CTC samples were assessed

for RNA expression using HyCEAD technology (ANGLE plc). Heatmaps were used to display the expression of individual genes for each patient. Genes identified during HyCEAD analysis were considered significantly upregulated if they had signal intensities of >20-fold higher than the average no-template control (NTC) gene amplification and were assigned a green color gradient (up to a change of 999-fold), with genes with signal intensities of ≥ 1000 -fold higher than NTC were assigned a red color gradient. Genes with signal intensities <20-fold higher than NTC were not considered significantly upregulated and were assigned a black color. HyCEAD HE chip analysis identified increased expression of genes (*green to red gradient*) in all three cohorts compared to NTC control, including (a) 48 genes in the LV-mHSPC cohort ($n = 7$ patients with CTCs); (b) 67 genes in the HV-mHSPC cohort ($n = 8$ patients with CTCs) and (c) 69 genes in the mCRPC cohort ($n = 9$ patients with CTCs).

HyCEAD chip analysis identifies differential expression of 9 biologically relevant genes which may contribute to prostate cancer progression

We were next interested in exploring the key gene expression differences between patient cohorts. Using a PubMed literature search of the biological relevance of transcripts displaying a > 20-fold increase in expression compared to healthy normal volunteers (HNV), we identified 3 genes whose lower expression has the potential to contribute to more advanced disease ([Table 2](#)). These genes had significantly higher expression in the LV-mHSPC cohort and lower expression in the HV-mHSPC and/or mCRPC cohorts. Additional analysis also identified 14 genes whose higher expression may contribute to more advanced disease ([Table 3](#)). These genes had significantly lower expression in the LV-mHSPC cohort and higher expression in the HV-mHSPC and/or mCRPC cohorts. Notably, 9 of the genes with differential expression in one or more patients between the cohorts have established links to EMT and/or invasive behavior, including NKX3-1, TOP2A, ERG, GHR, ITGBL1, NID2, ZNF217, VEGFA, and ST14 [[35](#)], [[36](#)], [[37](#)], [[38](#)], [[39](#)], [[40](#)], [[41](#)], [[42](#)], [[43](#)]].

Table 2. Expression/functional relevance of HyCEAD-identified genes that lose expression in CTCs with prostate cancer disease progression.

Gene name	Gene expression level/group (mean ± S.D.)			Loss of function contributes to cancer progression
	LV-HSPC	HV-HSPC	mCRPC	
Prostate Cancer (PC) chip				
NKX3-1*	15.2 ± 31.5	82.5 ± 232.5	5.4 ± 2.0	Tumor suppressor downregulated in metastatic prostate cancer [35]
FAM107A*	6.1 ± 17.7	3.9 ± 11.8	0 ± 0	Inhibits the progression of prostate cancer [45]
High Expression (HE) chip				
FERMT2*	17.0 ± 50.6	0 ± 0.1	0 ± 0.1	Tumor suppressor in ovarian cancer and colorectal cancer [46]

■ ≥2 patients/group with increased expression (amplification of >20 compared to no-template control (NTC))

□ 1 patient/group with increased expression (amplification of >20 compared to NTC)

■ 0 patients/group with increased expression (amplification of >20 compared to NTC)

* = finding supported by TCGA clinical data (*Supplemental Figure S3*)

Table 3. Expression/functional relevance of HyCEAD-identified genes that gain expression in CTCs with prostate cancer disease progression.

Gene name	Gene expression level/group (mean ± S.D.)			Gain of function contributes to cancer progression
	LV-HSPC	HV-HSPC	mCRPC	
Prostate cancer (PC) chip				
TOP2A*	5.1 ± 9.3	57.5 ± 131.3	7.8 ± 15.3	Associated with prostate cancer progression [47]
ERG*	4.7 ± 13.0	37.6 ± 58.4	28.9 ± 75.7	Overexpression promotes metastasis in prostate cancer [37]
CCNE2*	3.4 ± 2.0	38.0 ± 98.1	17.4 ± 25.1	Associated with poor prognosis in breast cancer [48]
GHR*	1.4 ± 1.0	27.7 ± 67.6	10.8 ± 30.5	Promotes growth/metastasis in pancreatic cancer [34]
VSTM2L*	1.3 ± 1.0	0.7 ± 0.4	5.3 ± 14.8	Associated with chemoresistance in rectal cancer [49]
ITGBL1*	0.8 ± 0.8	10.7 ± 28.9	4.9 ± 13.1	Promotes EMT, invasion and migration in prostate cancer [39]
High expression (HE) chip				
PIK3CA	44.6 ± 133.8	107.4 ± 213.5	112.7 ± 227.6	Increases cell division in prostate cancer [50]
NID2	24.4 ± 24.4	345.4 ± 489.0	153.2 ± 161.6	Linked to poor prognosis and invasion [40]
BARD1	22.8 ± 67.2	66.4 ± 141.1	75.6 ± 149.6	Isoforms are linked to poor outcomes [51]
CAV2	20.8 ± 62.0	276.4 ± 512.1	252.8 ± 564.1	Associated with prostate cancer progression [52]
ZNF217*	15.3 ± 44.9	155.6 ± 260.9	112.9 ± 152.0	Promotes prostate cancer tumor growth [54]
VEGFA	1.1 ± 0.8	97.7 ± 292.0	37.7 ± 74.2	Associated with tumor recurrence in prostate cancer [53]
TBP*	0.2 ± 0.3	29.7 ± 88.4	20.8 ± 61.3	Drives VEGFR expression in colon cancer [42]
ST14*	0.1 ± 0.1	135.1 ± 405.2	68.0 ± 134.4	Linked to breast cancer metastasis/poor survival [43]

■ ≥2 patients/group with increased expression (amplification of >20 compared to no-template control (NTC))

■ 1 patient/group with increased expression (amplification of >20 compared to NTC)

■ 0 patients/group with increased expression (amplification of >20 compared to NTC)

* = finding supported by TCGA clinical data (*Supplemental Figure S4*)

Finally, we examined the expression of genes identified by CTC HyCEAD analysis in our prostate patient cohorts relative to a larger patient dataset. We thus analyzed the 17 identified potentially biologically relevant genes using TCGA and UALCAN online clinical databases [33]. We observed significantly lower expression of 2 of the 3 identified HyCEAD downregulated genes (FAM107A and FERMT2) in primary prostate cancer patient tumors ($N = 497$) compared to normal prostatic samples ($N = 52$) ($p \leq 0.05$) (*Supplemental Figure S3a*). Additionally, these genes (FAM107A, FERMT2, and NKX3-1) had significantly lower expression in metastatic prostate cancer patients ($N = 44$) relative to non-metastatic prostate cancer patients ($N = 497$) ($p \leq 0.05$) (*Supplemental Figure S3b*). We also observed significantly higher expression of 8 of the 14 identified HyCEAD

upregulated genes (TOP2A, ERG, CCNE2, GHR, VSTM2L, ITGBL1, ST14, and ZNF217) in primary prostate cancer patient tumors ($N = 497$) compared to normal prostatic samples ($N = 52$) (*Supplemental Figure S4a*), with 3 genes (TOP2A, ERG, and CCNE2) also having significantly higher expression in metastatic prostate cancer patients ($N = 44$) relative to non-metastatic prostate cancer patients ($N = 497$) ($p \leq 0.05$) (*Supplemental Figure S4b*). Lastly, patients with high expression of TBP ($N = 125$) had decreased overall survival compared to patients with low expression of TBP ($N = 372$) ($p = 0.0038$) (*Supplemental Figure S4c*).

Discussion

Prostate cancer remains a leading cause of cancer diagnosis and cancer-related death in American men [1]. Most deaths from prostate cancer are due to metastatic, castrate-resistant disease, as current therapies are largely non-curative in this setting [2]. While the treatment landscape of advanced prostate cancer has been evolving with many available new treatment options based different molecular mechanisms, identifying optimal treatment sequencing to maximize chance of response while minimizing toxicity has been a key focus of current research in the field. There is therefore a clear need for new prognostic and predictive biomarkers such as CTCs to allow for more personalized treatment of prostate cancer patients.

The current pilot study assessed CTCs in metastatic prostate cancer patients at different disease progression stages along the spectrum of hormone-sensitive to castrate-resistant. We assessed CTCs from 29 prostate cancer patients using the epithelial-based CellSearch and the EMT-independent Parsortix CTC analysis platforms. The earliest cohort examined was LV-mHSPC [29], the “middle” cohort was HV-mHSPC [29], and the most advanced cohort was mCRPC [30]. We originally hypothesized that as disease became more advanced, we would observe a greater number of CTCs overall, as well as increased CTC capture by the EMT-independent Parsortix compared to the epithelial-based CellSearch based on a predicted evolution of CTCs to a more mesenchymal phenotype. However, unexpectedly and contradictory to our hypothesis, we did not see any significant differences in CTC enumeration between technologies within any of the patient cohorts. This highlights that Parsortix can capture and enumerate CTCs just as effectively as CellSearch; the most established FDA-approved CTC analysis platform [8]. We also assessed differences in CTC enumeration between the three progressive patient cohorts and observed significantly greater CTC numbers in the HV-mHSPC cohort relative to the LV-mHSPC cohort using CellSearch. Although this result contrasted with our original hypothesis, it does highlight the ability of both platforms to capture CTCs throughout disease progression, particularly as disease burden increases. This significant difference in CTCs between LV-mHSPC versus HV-mHSPC patients, along with the observed trend towards detection of higher CTCs in HV-mHSPC and mCRPC patients with

CellSearch versus Parsortix may also be explained by previous studies that have demonstrated that CTCs with a hybrid epithelial-mesenchymal phenotype are still detectable by CellSearch and are indicative of poor prognosis [12,[21], [22], [23]]. Taken together, our findings therefore provide support for the continued clinical use of CellSearch for enumeration of CTCs in prostate cancer patients across the spectrum of hormone sensitivity and metastatic progression.

The observation that the HV-mHSPC cohort (versus the more advanced mCRPC cohort) had the greatest number of CTCs was also somewhat unexpected and provided a rationale for further CTC analysis at the molecular level, something which is more feasible with Parsortix versus CellSearch [8]. Indeed, the Parsortix platform was recently FDA-approved for the isolation of CTCs for subsequent downstream analysis in metastatic breast cancer. Assessing patient CTCs is becoming increasingly more important within the context of personalized medicine and advancing the utility of CTC research [44]. In support of this, ANGLE plc developed a novel RNA analysis approach that can be used in conjunction with the Parsortix CTC harvest protocol. This HyCEAD mRNA assay uses hybrid capture and amplification of targeted genes combined with flow-through array multiplex detection (Ziplex) to assess up to 100 genes/chip with detection of specific genes in as few as 1 CTC per sample [27,28]. In the current study, we used HyCEAD to assess the expression of 155 genes in CTC populations from our 3 patient cohorts using two analysis chips (PC and HE). Interesting, consistent with the higher CTC counts observed in the HV-HSPC cohort, the gene expression studies revealed both the greatest heterogeneity of gene expression changes between patients and the greatest number of total altered genes in the HV-mHSPC cohort, suggesting the possibility that comprehensive CTC analysis in this “middle” stage of metastatic prostate cancer progression might provide particularly valuable information to inform treatment decision-making.

Using pooled analysis of the data from these two chips, we were able to identify a total of 119 genes with altered expression among the 3 patient cohorts. Importantly, 3 of the genes that demonstrated lower expression as disease cohorts became more advanced (NKX3-1, FAM107A, and FERMT2) have previously been shown to have a loss-of-function during cancer progression [35,45,46]. Additionally, 14 of the genes that demonstrated higher expression as disease cohorts became more advanced (TOP2A, ERG, CCNE2, GHR, VSTM2L, ITGBL1, PIK3CA, NID2, BARD1, CAV2, ZNF217, VEGFA, TBP, and ST14) have been associated with a gain-of-function as cancer progresses [[37], [38], [39], [40], [41], [42], [43],[47], [48], [49], [50], [51], [52], [53]]. We then further validated these 14 potentially biologically significant genes in a larger cohort of prostate cancer patient tissues samples using the TCGA online database. We observed that 2 of 3 of the identified lower expression HyCEAD genes (FAM107A and FERMT2) have decreased expression in prostate tumor tissue compared to normal prostatic tissue, with FAM107A, FERMT2, and NKX3-1

also having decreased expression in metastatic prostate cancer compared to primary tumors. Similarly, of the genes that HyCEAD identified as having higher expression in the more advanced cohorts, 8 of 14 genes (TOP2A, ERG, CCNE2, GHR, VSTM2L, ITGB1, ST14, and ZNF217) were validated through TCGA as having increased expression in prostate tumor tissue compared to normal tissue. TOP2A, ERG, and CCNE2 also had higher expression in metastatic prostate cancer compared to primary tumors, and increased TBP expression was correlated with decreased overall survival. These observations are also supported by previous prospective studies in mCRPC patients using HyCEAD and the PC Chip, which demonstrated a correlation between increased TOP2A and ERG in CTCs and decreased progression-free and overall survival [28].

Notably, 9 of the identified HyCEAD genes with differential expression between cohorts have been identified within the literature as being involved in processes that promote cancer aggressiveness including EMT and partial-EMT, metastasis, invasion, proliferation and cell motility. Specifically, NKX3-1 has been shown to be a prostatic tumor suppressor gene and a marker of metastatic prostate cancer carcinoma [35]. TOP2A has been shown to promote cell migration, invasion, and EMT in cervical cancer [36]. ERG is associated with prostate cancer progression through gene fusion in the promoter region of the androgen-induced TMPRSS2 gene [37]. GHR has been shown to induce molecular mechanisms that cause EMT [38]. ITGBL1 has been shown to promote EMT, invasion, and migration in prostate cancer. NID2 promotes invasion and migration in gastric cancer [40]. ZNF217 is associated with invasion, metastasis, and EMT [54]. VEGFA increases motility, and invasion through Slug induction in breast cancer cells [55]. Lastly, ST14 is involved in the metastasis of breast cancer and poor survival [43]. HyCEAD analysis of CTCs in this study revealed substantial differences within and between metastatic patient cohorts which was not apparent through CTC enumeration alone. This underscores the importance of downstream molecular CTC characterization for providing oncologists with more information about their patients' disease; including the involvement of EMT, its impact on disease progression, and the resulting implications for personalized medicine.

Despite identifying several meaningful findings, we acknowledge that our study has the inherent limitation of being designed as a proof-of-principle pilot clinical study, and thus by its nature it had a small size ($N = 29$). This resulted in an inability to meaningfully analyze correlations between CTC counts, CTC gene expression, and clinical status. A larger follow-up clinical study that is appropriately powered to allow correlative analysis of CTC enumeration, CTC gene expression, and clinical outcomes in LV-mHSPC, HV-mHSPC and mCRPC patients is planned for the future in order to address this limitation.

In summary, the results of this study support the continued clinical use of CellSearch for enumerating CTCs in all progression stages of metastatic prostate cancer. Our findings

also highlight the value of combined implementation of Parsortix and HyCEAD for CTC enumeration, harvest, and downstream analysis. In particular, the molecular characterization of CTCs in this study provides a promising panel of potential biomarkers for further investigation to develop a comprehensive, real-time CTC liquid biopsy strategy personalized clinical management of metastatic prostate cancer patients in the future.

Data availability

The datasets generated and analyzed during the current study are available from the corresponding author upon request.

Funding sources

This research was funded by a Movember Discovery Grant from Prostate Cancer Canada (grant # [D2017-1974](#)). J.K. was the recipient of a scholarship from the Lawson Health Research Institute (IRF Award) and the Province of Ontario (Ontario Graduate Scholarship).

CRedit authorship contribution statement

Jenna Kitz: Conceptualization, Data curation, Formal analysis, Investigation, Methodology, Validation, Visualization, Writing – original draft, Writing – review & editing. **Kelly Seto:** Formal analysis, Methodology, Validation, Writing – review & editing. **Pinki Nandi:** Formal analysis, Methodology, Validation, Writing – review & editing. **Paul Smith:** Formal analysis, Methodology, Validation, Writing – review & editing. **David Englert:** Formal analysis, Methodology, Validation, Writing – review & editing. **Ayten Hijazi:** Investigation, Validation, Writing – review & editing. **Michael Lock:** Investigation, Resources, Writing – review & editing. **Glenn S. Bauman:** Investigation, Resources, Writing – review & editing. **Scott Ernst:** Investigation, Resources, Writing – review & editing. **Ricardo Fernandes:** Investigation, Resources, Writing – review & editing. **Alison L. Allan:** Conceptualization, Data curation, Formal analysis, Funding acquisition, Methodology, Project administration, Resources, Supervision, Visualization, Writing – review & editing.

Declaration of competing interest

The authors declare the following financial interests/personal relationships which may be considered as potential competing interests: Alison L Allan reports financial support was provided by Prostate Cancer Canada. Kelly Seto, Pinki Nandi, Paul Smith, David Englert reports a relationship with ANGLE Biosciences Inc., Toronto, ON, Canada that

includes: employment. Glenn S. Bauman reports a relationship with Novartis, Advanced Accelerator Applications and the Ontario Institute for Cancer Research that includes: consulting or advisory. Ricardo Fernandes reports a relationship with Merck, Novartis, Ipsen, Janssen, Pfizer, BMS, and Bayer that includes: consulting or advisory and travel reimbursement. All other authors declare no competing interests. If there are other authors, they declare that they have no known competing financial interests or personal relationships that could have appeared to influence the work reported in this paper.

Acknowledgements

We gratefully acknowledge all the prostate cancer patients who were willing to provide informed consent and participate in this study. We thank Kes Sebborn and Joseph Andrews who provided valuable assistance with clinical study administration, patient recruitment and consent, and clinical data management through the London Health Sciences Centre Cancer Clinical Trials Unit. Finally, we thank members of our laboratory group for their assistance with sample receiving and shipping and for consenting to serve as healthy normal donors for our initial HyCEAD validation studies.

Appendix. Supplementary materials

 [Download: Download Acrobat PDF file \(577KB\)](#)

[Recommended articles](#)

References

- [1] R.L. Siegel, K.D. Miller, N.S. Wagle, A. Jemal
Cancer statistics, 2023
CA Cancer J. Clin., 73 (2023), pp. 17-48
[Crossref ↗](#) [View in Scopus ↗](#) [Google Scholar ↗](#)
- [2] A.F. Chambers, A.C. Groom, I.C. MacDonald
Dissemination and growth of cancer cells in metastatic sites
Nat. Rev. Cancer, 2 (2002), pp. 563-572
[Crossref ↗](#) [View in Scopus ↗](#) [Google Scholar ↗](#)
- [3] H. Lilja, D. Ulmert, A.J. Vickers
Prostate-specific antigen and prostate cancer: prediction, detection and monitoring
Nat. Rev. Cancer, 8 (2008), pp. 268-278
[Crossref ↗](#) [View in Scopus ↗](#) [Google Scholar ↗](#)

- [4] J.S. De Bono, *et al.*
Circulating tumor cells predict survival benefit from treatment in metastatic castration-resistant prostate cancer
Clin. Cancer Res., 14 (2008), pp. 302-309
[Google Scholar ↗](#)
- [5] A. Goldkorn, *et al.*
Circulating tumor cell counts are prognostic of overall survival in SWOG S0421: a phase III trial of docetaxel with or without atrasentan for metastatic castration-resistant prostate cancer
J. Clin. Oncol., 32 (2014), pp. 1136-1142
[View in Scopus ↗](#) [Google Scholar ↗](#)
- [6] A.L. Allan, M. Keeney
Circulating tumor cell analysis: technical and statistical considerations for application to the clinic
J. Oncol., 2010 (2010), Article 426218
[View in Scopus ↗](#) [Google Scholar ↗](#)
- [7] Menarini Silicon Biosystems
CellSearch CTC Test. (2024)
<https://www.cellsearchctc.com/> ↗
[Google Scholar ↗](#)
- [8] L.E. Lowes, A.L. Allan
Recent advances in the molecular characterization of circulating tumor cells
Cancers (Basel), 16 (2014), pp. 595-624
[Crossref ↗](#) [View in Scopus ↗](#) [Google Scholar ↗](#)
- [9] W.J. Allard, *et al.*
Tumor cells circulate in the peripheral blood of all major carcinomas but not in healthy subjects or patients with nonmalignant diseases
Clin. Cancer Res., 10 (2004), pp. 6897-6904
[View in Scopus ↗](#) [Google Scholar ↗](#)
- [10] J.T. Nauseef, M.D. Henry
Epithelial-to-mesenchymal transition in prostate cancer: paradigm or puzzle?
Nat. Rev. Urol., 8 (2011), pp. 428-439
[Crossref ↗](#) [View in Scopus ↗](#) [Google Scholar ↗](#)

- [11] J.P. Thiery, H. Acloque, R.Y.J. Huang, M.A. Nieto
Epithelial-mesenchymal transitions in development and disease
Cell, 139 (2009), pp. 871-890
 [View PDF](#) [View article](#) [View in Scopus ↗](#) [Google Scholar ↗](#)
- [12] M.K. Jolly, *et al.*
Implications of the hybrid epithelial/mesenchymal phenotype in metastasis
Front. Oncol., 20 (2015), p. 155
[View in Scopus ↗](#) [Google Scholar ↗](#)
- [13] D. Gleason
Classification of prostatic carcinomas
Cancer Chemother. Rep., 50 (1966), pp. 125-128
[View in Scopus ↗](#) [Google Scholar ↗](#)
- [14] H.E. Schaafsma, P.P. Bringuier, G.O.N. Oosterhof, F.M.J. Debruyne, J.A. Schalken
Decreased E-Cadherin expression is associated with poor prognosis in patients with prostate cancer
Cancer Res, 54 (1994), pp. 3929-3933
[Google Scholar ↗](#)
- [15] M. Jaggi, *et al.*
N-cadherin switching occurs in high Gleason grade prostate cancer
Prostate, 66 (2006), pp. 193-199
[Crossref ↗](#) [View in Scopus ↗](#) [Google Scholar ↗](#)
- [16] S.H. Lang, *et al.*
Enhanced expression of vimentin in motile prostate cell lines and in poorly differentiated and metastatic prostate carcinoma
Prostate, 52 (2002), pp. 253-263
[View in Scopus ↗](#) [Google Scholar ↗](#)
- [17] C.E. Poblete, *et al.*
Increased SNAIL expression and low syndecan levels are associated with high Gleason grade in prostate cancer
Int. J. Oncol., 44 (2014), pp. 647-654
[Crossref ↗](#) [View in Scopus ↗](#) [Google Scholar ↗](#)
- [18] Y. Sun, *et al.*
Androgen deprivation causes epithelial-mesenchymal transition in the prostate: implications for androgen-deprivation therapy

Cancer Res, 72 (2012), pp. 527-536

[View in Scopus ↗](#) [Google Scholar ↗](#)

- [19] K. Jennbacken, T. Tešan, W. Wang, H. Gustavsson, J.E. Damber, K. Welén
N-cadherin increases after androgen deprivation and is associated with metastasis in prostate cancer

Endocr. Relat. Cancer, 17 (2010), pp. 469-479

[View in Scopus ↗](#) [Google Scholar ↗](#)

- [20] L. Miao, *et al.*
Disrupting androgen receptor signaling induces snail-mediated epithelial-mesenchymal plasticity in prostate cancer

Cancer Res, 77 (2017), pp. 3101-3112

[View in Scopus ↗](#) [Google Scholar ↗](#)

- [21] A.J. Armstrong, *et al.*
Circulating tumor cells from patients with advanced prostate and breast cancer display both epithelial and mesenchymal markers

Mol. Cancer Res., 9 (2011), pp. 997-1007

[View in Scopus ↗](#) [Google Scholar ↗](#)

- [22] T.M. Gorges, *et al.*
Circulating tumour cells escape from EpCAM-based detection due to epithelial-to-mesenchymal transition

BMC Cancer, 12 (2012), p. 178

[View in Scopus ↗](#) [Google Scholar ↗](#)

- [23] C.R. Lindsay, *et al.*
Vimentin and Ki67 expression in circulating tumour cells derived from castrate-resistant prostate cancer

BMC Cancer, 16 (2016), p. 168

[View in Scopus ↗](#) [Google Scholar ↗](#)

- [24] L.E. Lowes, *et al.*
Epithelial-to-mesenchymal transition leads to disease-stage differences in circulating tumor cell detection and metastasis in pre-clinical models of prostate cancer

Oncotarget, 7 (2016), pp. 76125-76139

[Crossref ↗](#) [View in Scopus ↗](#) [Google Scholar ↗](#)

- [25] G.E. Hvichia, *et al.*
A novel microfluidic platform for size and deformability based separation and the subsequent molecular characterization of viable circulating

tumor cells

Int. J. Cancer, 138 (2016), pp. 2894-2904

[Crossref ↗](#) [View in Scopus ↗](#) [Google Scholar ↗](#)

[26]

L. Xu, *et al.*

Optimization and evaluation of a novel size based circulating tumor cell isolation system

PLoS One, 10 (2015), Article e0138032

[Crossref ↗](#) [View in Scopus ↗](#) [Google Scholar ↗](#)

[27]

D.F. Englert, *et al.*

Multiplex gene expression using the HyCEAD assay in CTCs isolated with the Parsortix system

Cancer Res, 79 (13_Supplement) (2019), p. 1375

[Google Scholar ↗](#)

[28]

L. Groen, *et al.*

Transcriptome profiling of circulating tumor cells to predict clinical outcomes in metastatic castration-resistant prostate cancer

Int. J. Mol. Sci., 24 (2023), p. 9002

[Crossref ↗](#) [View in Scopus ↗](#) [Google Scholar ↗](#)

[29]

C.J. Sweeney, *et al.*

Chemohormonal therapy in metastatic hormone-sensitive prostate cancer

N. Engl. J. Med., 373 (2015), pp. 737-746

[View in Scopus ↗](#) [Google Scholar ↗](#)

[30]

H.I. Scher, M.J. Morris, E. Basch, G. Heller

End points and outcomes in castration-resistant prostate cancer: from clinical trials to clinical practice

J. Clin. Oncol., 29 (2011), pp. 3695-3704

[View in Scopus ↗](#) [Google Scholar ↗](#)

[31]

L.E. Lowes, *et al.*

The significance of circulating tumor cells in prostate cancer patients undergoing adjuvant or salvage radiation therapy

Prostate Cancer Prostatic Dis, 18 (2015), pp. 358-864

[Crossref ↗](#) [View in Scopus ↗](#) [Google Scholar ↗](#)

[32]

J. Kitz, D. Goodale, C. Postenka, L.E. Lowes, A.L. Allan

EMT-independent detection of circulating tumor cells in human blood samples and pre-clinical mouse models of metastasis

Clin. Exp. Metastasis., 38 (2021), pp. 97-108

[Crossref ↗](#) [View in Scopus ↗](#) [Google Scholar ↗](#)

[33]

D.S. Chandrashekar, *et al.*

UALCAN: a portal for facilitating tumor subgroup gene expression and survival analyses

Neoplasia, 19 (2017), pp. 649-658



[View PDF](#)

[View article](#)

[View in Scopus ↗](#)

[Google Scholar ↗](#)

[34]

P. Msaouel, N. Pissimissis, A. Halapas, M. Koutsilieris

Mechanisms of bone metastasis in prostate cancer: clinical implications

Best Pract. Res. Clin. Endocrinol. Metab., 22 (2008), pp. 341-355



[View PDF](#)

[View article](#)

[View in Scopus ↗](#)

[Google Scholar ↗](#)

[35]

B. Gurel, *et al.*

NKX3.1 as a marker of prostatic origin in metastatic tumors

Am. J. Surg. Pathol., 34 (2010), pp. 1097-1105

[View in Scopus ↗](#)

[Google Scholar ↗](#)

[36]

B. Wang, *et al.*

TOP2A promotes cell migration, invasion and epithelial-mesenchymal transition in cervical cancer via activating the PI3K/AKT signaling

Cancer Manag. Res., 12 (2020), pp. 3807-3814

[Crossref ↗](#)

[View in Scopus ↗](#)

[Google Scholar ↗](#)

[37]

P. Adamo, M.R. Ladomery

The oncogene ERG: a key factor in prostate cancer

Oncogene, 35 (2016), pp. 403-414

[Crossref ↗](#)

[View in Scopus ↗](#)

[Google Scholar ↗](#)

[38]

R. Subramani, *et al.*

Growth hormone receptor inhibition decreases the growth and metastasis of pancreatic ductal adenocarcinoma

Exp. Mol. Med., 46 (2014), pp. 1-11

[View in Scopus ↗](#)

[Google Scholar ↗](#)

[39]

W. Li, S. Li, J. Yang, C. Cui, M. Yu, Y. Zhang

ITGBL1 promotes EMT, invasion and migration by activating NF- κ b signaling pathway in prostate cancer

Onco. Targets Ther., 12 (2019), pp. 3753-3763

[Crossref ↗](#)

[View in Scopus ↗](#)

[Google Scholar ↗](#)

- [40] Yu, Z., et al. NID2 can serve as a potential prognosis prediction biomarker and promotes the invasion and migration of gastric cancer. *Pathol. Res. Pract.* 215, 152553.
[Google Scholar ↗](#)
- [41] X. Jiang, et al.
Elevated expression of ZNF217 promotes prostate cancer growth by restraining ferroportin-conducted iron egress
Oncotarget, 7 (2016), pp. 84893-84906
[Crossref ↗](#) [View in Scopus ↗](#) [Google Scholar ↗](#)
- [42] Johnson, S.A.S., Lin, J.J., Walkey, C.J., Leathers, M.P., Coarfa, C., & Johnson, D.L.
Elevated TATA-binding protein expression drives vascular endothelial growth factor expression in colon cancer. *Oncotarget*. 8, 48832–48845.
[Google Scholar ↗](#)
- [43] K.Y. Kim, et al.
Targeting metastatic breast cancer with peptide epitopes derived from autocatalytic loop of Prss14/ST14 membrane serine protease and with monoclonal antibodies
J. Exp. Clin. Cancer Res., 38 (2019), p. 363
[Google Scholar ↗](#)
- [44] A. Toss, Z. Mu, S. Fernandez, M. Cristofanilli
CTC enumeration and characterization: moving toward personalized medicine
Ann. Transl. Med., 2 (2014), p. 108
[View in Scopus ↗](#) [Google Scholar ↗](#)
- [45] H. Nakajima, K. Koizumi
Family with sequence similarity 107: a family of stress responsive small proteins with diverse functions in cancer and the nervous system
(Review)
Biomed. Rep., 2 (2014), pp. 321-325
[Crossref ↗](#) [Google Scholar ↗](#)
- [46] X. Su, et al.
Comprehensive analysis of prognostic value and immune infiltration of kindlin family members in non-small cell lung cancer
BMC Med. Genomics, 14 (2021), p. 119
[View in Scopus ↗](#) [Google Scholar ↗](#)

- [47] J.L. Schaefer-Klein, S.J. Murphy, S.H. Johnson, G. Vasmatzis, I.V. Kovtun
Topoisomerase 2 alpha cooperates with androgen receptor to contribute to prostate cancer progression
PLoS One, 10 (2015), pp. 1-17
[Google Scholar ↗](#)
- [48] C. Lee, *et al.*
Cyclin E2 promotes whole genome doubling in breast cancer
Cancers (Basel), 12 (2020), pp. 1-19
[Google Scholar ↗](#)
- [49] H. Liu, Z. Zhang, P. Zhen, M. Zhou
High expression of VSTM2L induced resistance to chemoradiotherapy in rectal cancer through downstream IL-4 signaling
J. Immunol. Res., 2021 (2021), Article 6657012
[View in Scopus ↗](#) [Google Scholar ↗](#)
- [50] Z. García, A. Kumar, M. Marqués, I. Cortés, A.C. Carrera
Phosphoinositide 3-kinase controls early and late events in mammalian cell division
EMBO J, 25 (2006), pp. 655-661
[Crossref ↗](#) [View in Scopus ↗](#) [Google Scholar ↗](#)
- [51] M. Ratajska, *et al.*
Cancer predisposing BARD1 mutations affect exon skipping and are associated with overexpression of specific BARD1 isoforms
Oncol. Rep., 34 (2015), pp. 2609-2917
[Crossref ↗](#) [View in Scopus ↗](#) [Google Scholar ↗](#)
- [52] S. Sugie, S. Mukai, K. Yamasaki, T. Kamibeppu, H. Tsukino, T. Kamoto
Significant association of caveolin-1 and caveolin-2 with prostate cancer progression
Cancer Genomics Proteomics, 12 (2015), pp. 391-396
[View in Scopus ↗](#) [Google Scholar ↗](#)
- [53] Y. Nordby, *et al.*
Stromal expression of VEGF-A and VEGFR-2 in prostate tissue is associated with biochemical and clinical recurrence after radical prostatectomy
Prostate, 75 (2015), pp. 1682-1693
[Crossref ↗](#) [View in Scopus ↗](#) [Google Scholar ↗](#)

- [54] P.A. Cohen, C.F. Donini, N.T. Nguyen, H. Lincet, J.A. Vendrell
The dark side of ZNF217, a key regulator of tumorigenesis with powerful
biomarker value

Oncotarget, 6 (2015), pp. 41566-41581

[Crossref ↗](#) [View in Scopus ↗](#) [Google Scholar ↗](#)

- [55] M. Kim, *et al.*
VEGFA links self-renewal and metastasis by inducing Sox2 to repress
miR-452, driving slug

Oncogene, 36 (2017), pp. 5199-5211

[Crossref ↗](#) [View in Scopus ↗](#) [Google Scholar ↗](#)

Cited by (0)

© 2025 The Authors. Published by Elsevier Ltd.



All content on this site: Copyright © 2025 Elsevier B.V., its licensors, and contributors. All rights are reserved, including those for text and data mining, AI training, and similar technologies. For all open access content, the relevant licensing terms apply.

